JOURNAL OF OPTOELECTRONICS AND ADVANCED MATERIALS Vol. 8, No. 1, February 2006, p. 191 - 196

Spin density calculations for two electron-acceptor constituents of molecular magnets: tetracyanoethylene and hexacyanobutadiene

C. I. OPREA, A. DAMIAN[a], M. A. GÎRȚU[a*]
Laboratory of Theoretical Chemistry, Royal Institute of Technology, Stockholm, Sweden
[a]Department of Physics, Ovidius University, Constanta, Romania

We report quantum chemical calculations providing the spin density of two molecules used as building blocks for molecular magnets: tetracyanoethylene (TCNE) and hexacyanobutadiane (HCBD). Very good electron-acceptors, both molecules are used as building blocks of novel, nanostructured charge-transfer salts with magnetic properties. We investigate by means of perturbation theory (MP2) and density functional theory (DFT) the electronic structure of the neutral molecules as well as of the anionic radicals, and we discuss the roles of the various factors influencing the electron-accepting properties of these molecules. We compare and contrast the charge-acceptor and magnetic properties of both molecules, based on the correlation between their structures, electronic spectrum and spin densities.

(Received October 14, 2005; accepted January 26, 2006)

Keywords: Molecular magnets, Charge transfer salts, Density functional theory, Perturbation theory, Electron affinity, Spin density

1. Introduction

Electron-donor and electron-acceptor molecules determined recently a high interest as they are key constituents of novel molecular materials with unusual magnetic and conducting properties [1, 2]. The characterization of the electronic spectrum of such species is a crucial step for the understanding of the properties exhibited by the systems in which they take part, as well as for the design of novel materials with enhanced characteristics, such as charge-transfer salts with magnetic properties.

Tetracyanoethylene (TCNE) is one of the most powerful organic electron acceptors, being a prototype for other cyano-based electron acceptors such as hexacyanobutadiene (HCBD) and tetracyanoquinodimethane (TCNQ). While TCNE is a basic constituent in charge transfer compounds with either magnetic or conducting properties [1,2], HCBD has been used in building hybrid organic-inorganic molecular magnets [3]. An example in which both molecules occur is the family of manganese porphyrin-based magnets [4], which are charge-transfer salts consisting of linear chains of electron-donor manganese porphyrins (such as Mn-octaethylporphyrin, MnOEP, or Mn-tetraphenylporphyrin; MnTPP) trans-μ bounded to electron-acceptor cyano-based ligands (such as TCNE and HCBD). The family of metalloporphyrin-based magnets had provided [4] an unusual opportunity for the study of magnetic ordering because it offers a wide range of controlling factors. For instance, the cyanocarbon bridge connecting the adjacent porphyrins was shown to influence the intrachain interaction [4]. Recent progress made in understanding the role of the building blocks forming these materials revealed interesting magnetic properties (one-dimensional ferrimagnetic behavior at high temperatures, three dimensional canted antiferromagnetic or weak ferromagnetic behavior at low temperatures) [5], and phenomena (spin- and/or lattice-dimensionality crossovers [6] or cluster-glass-like relaxation processes [7]).

The paper reports quantum chemical calculations for the determination of the electronic structure and electron affinity of TCNE and HCBD molecules as well as of the spin density of the corresponding anionic radicals. For these calculations we use perturbation theory (MP2) and density functional theory (DFT).

As the accurate calculation of the electron affinity of electron acceptors requires considerable computational efforts (because of the mandatory use of large electron basis sets and of a balanced incorporation of electron correlation effects [8, 9]), density functional theory (DFT) methods have emerged as promising computational techniques. It was shown [9] that DFT methods can be successfully applied to determine molecular electron affinities at a low computational cost, and, in most cases, the predicted values are within 0.2 eV or better of the experimental values.

The electron affinity of TCNE has been determined experimentally to be 3.17 ± 0.2 eV [10], while previous results led to 2.89 eV [11]. Recently, it was argued [12] that DFT calculations overestimate this value by about 0.5 eV and alternative solutions proposed were the taking into account of structure twisting or the use of coupled cluster (CC) computational techniques [13]. CC methods have proven to be accurate but their use is severely hampered by computational limitations [14,15].

2. Computational details

Geometrical parameters, electron affinities and spin densities were computed using density functional theory (DFT) and second-order Møller-Plesset perturbation theory (MP2). For the DFT calculations, the B3LYP hybrid functional has been employed [16,17]. It has been shown that this hybrid functional is an excellent choice because it properly reproduces structural parameters of cyano-substituted ethylenes [9,13]. The calculations have been performed with the correlation-consistent cc-pVDZ [18] set on GAUSSIAN 03 [19]. The geometry optimization was performed using D2h symmetry, as both the neutral TCNE molecule and the anionic radical posses planar molecular structure [20, 21]. Adiabatic electron affinities were calculated as the energy difference between the neutral molecule and the anion at their respective optimized geometries. The geometrical structure and the molecular orbitals (MO) were examined and displayed using MOLDEN [22].

3. Results and discussion

3.1 Neutral and reduced TCNE

The optimized geometrical calculations of neutral and reduced TCNE compare well with experimental [21, 23, 24] as well as simulation [15, 25] results. Table 1 shows that both DFT and MP2 reveal that the structural parameters of TCNE change significantly after accepting an electron. The distance the most affected is r_1, the one between the two central carbon atoms, which increase, just like r_3, the one between C and N in the cyano group, while the distance r_2, between the central carbons and the nearest carbon atom in a cyano group shortens (see Fig. 1).

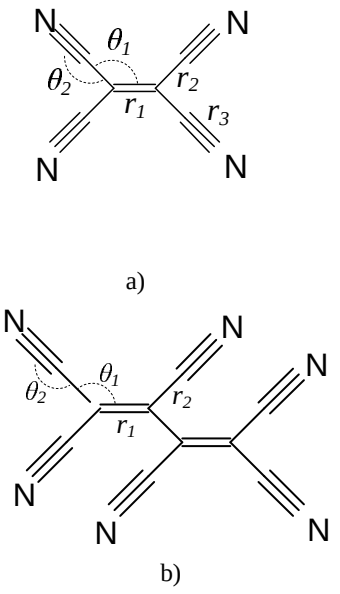

Fig. 1. Structural parameters of TCNE (a) and HCBD (b).

Table 1. Geometrical parameters of TCNE and TCNE.- optimized by DFT and MP2. The units are Å for the bond lengths and degrees for the bond angles.

Parameter	Species	Method	
		MP2/ cc-pVDZ	B3LYP/ cc-pVDZ
r_1 (C=C)	Neutral	1.381	1.373
	Anion	1.440	1.443
r_2 (C–C)	Neutral	1.437	1.432
	Anion	1.426	1.416
r_3 (C≡N)	Neutral	1.191	1.164
	Anion	1.164	1.172
θ_1 (C–C=C)	Neutral	120.9	121.5
	Anion	121.0	121.6
θ_2 (C–C≡N)	Neutral	179.8	179.0
	Anion	179.6	179.3

The energy spectrum calculations were performed for TCNE and $TCNE^{\cdot-}$, the results for the highest occupied molecular orbital (HOMO) and lowest unoccupied molecular orbital (LUMO) being shown in Table 2 and Fig. 2. The analysis of the HOMO and LUMO orbitals for TCNE and $TCNE^{\cdot-}$ explains the differences between the geometrical parameters of the two systems.

The HOMO of TCNE (shown in Fig. 2a) has shorter inter-atomic distances between the two central carbon atoms (C==C) and between the carbon and nitrogen of each cyano group (C≡≡N) because of the bonding character of those bonds. The nodal planes present between the central carbon atoms and the carbons of the cyano groups lead to longer distances between such atoms.

The LUMO of TCNE has a very different topology (Fig. 2b), with nodal planes where the HOMO has bonds and bonds where the HOMO has nodes. The LUMO has antibonding character over the C==C and C≡≡N bonds and bonding character over the C—C bonds, determining a lengthening of the r_1 and r_3 distances and a shortening of the r_2 distance.

Whereas both DFT and MP2 have led so far to similar qualitative results, in the case of the next lowest unoccupied MO of TCNE the two methods give very different topologies (Fig. 2c and 2d). DFT indicates the presence of a median nodal plane, while MP2 suggests, on the contrary, a strong bonding between both the central carbons and the carbons involved in cyano groups.

In the case of the anionic radical $TCNE^{\cdot-}$ the single occupied MO (SOMO) corresponds to the LUMO of the TCNE molecule. In this case, however, the presence of a net spin leads to a difference between the energies for the spin up (alpha) and spin down (beta) states. DFT and MP2 give similar results for both the HOMO and the SOMO, results that are very much alike with the HOMO and LUMO of TCNE. Again, differences occur when looking further, at the LUMO of $TCNE^{\cdot-}$, where DFT and MP2 give different results, and again these results correspond to those obtained for TCNE.

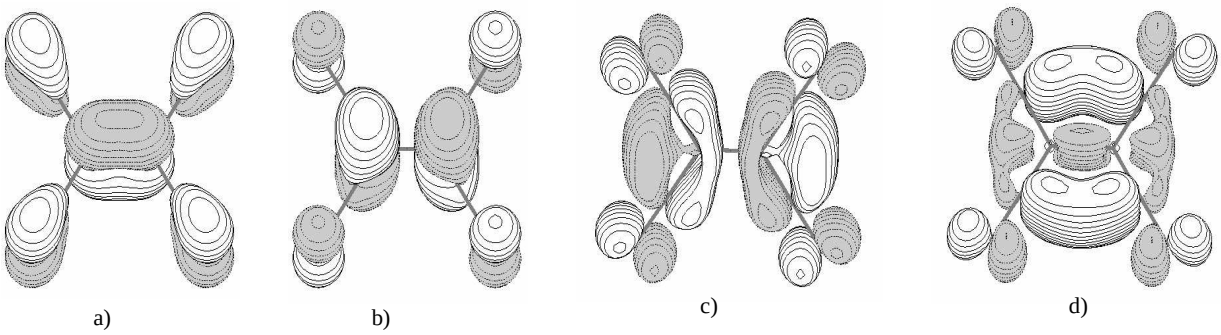

Fig. 2. Electronic density contours (0.05 e/bohr^3) for the highest occupied MO (a), lowest unoccupied MO (b), and next lowest unoccupied MO of TCNE, calculated with DFT (c) and with MP2 (d).

Moving from qualitative to quantitative differences between the two methods, we note that, clear differences occur between the energy values, as it can be seen from Table 2. For instance, compared to DFT results, the MP2 value for the HOMO energy of TCNE is lower while for the LUMO energy is higher.

Table 2. Energies for most relevant MOs of neutral and reduced TCNE (in Hartree).

Method / Molecule		DFT (cc-pVDZ)			MP2 (cc-pVDZ)	
TCNE	HOMO	-0.33640		HOMO	-0.43112	
	LUMO	-0.18329		LUMO	-0.06684	
	next LUMO	-0.06770		next LUMO	0.08099	
$TCNE^{\cdot-}$		alpha	beta		alpha	beta
	HOMO	-0.14253	-0.11265	HOMO	-0.29204	-0.18242
	SOMO	-0.04429	0.02928	SOMO	-0.15781	0.17598
	LUMO	0.12777	0.13075	LUMO	0.28661	0.29796

Adiabatic electron affinities were calculated as the energy difference between the neutral molecule and the anionic radical. While the experimental value is 3.17 eV [10], the calculated values are 1.70 eV with MP2/cc-pVDZ and 3.10 eV with DFT/cc-pVDZ, in accordance with other theoretical results [15].

To understand the spin coupling mechanism that leads to cooperative magnetic behavior of TCNE-based molecular magnets it is important to determine the spin distribution of the anionic radical $TCNE^{\cdot-}$. In this respect, both DFT and MP2 calculations have provided similar qualitative results (as shown in Table 3 and Fig. 3), with the largest spin density on the central carbon atoms and relatively large values (and similar spin orientation) on the nitrogen atoms. An opposite orientation spin density is located on the carbon atoms that belong to the cyano groups and in the space adjacent to the central carbons.

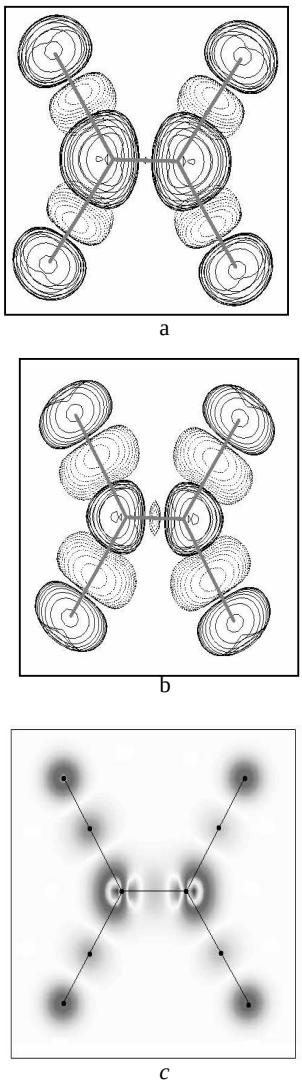

Fig. 3. Spin density contours (0.001 μ_B/bohr^3) of the SOMO of $TCNE^{\cdot-}$ obtained by means of DFT (a) and MP2 (b) calculations. Experimental spin density based on neutron diffraction measurements, from ref. [21] (c).

Table 3. Calculated and experimental (see ref. [21]) spin density values for the anionic radical $TCNE^{\cdot-}$. The values in the last column are obtained based on those in the previous one by scaling the experimental net spin to one.

Index	Atom	Spin density value			
		DFT	MP2	Exp	Exp (norm)
1	C	0.316757	0.471826	0.255	0.335
2	C	0.316768	0.471766	0.255	0.335
3	C	-0.071667	-0.427901	-0.040	-0.0525
4	C	-0.071670	-0.427868	-0.030	-0.0394
5	C	-0.071667	-0.427901	-0.025	-0.0328
6	C	-0.071670	-0.427868	-0.057	-0.0749
7	N	0.163284	0.442003	0.095	0.125
8	N	0.163291	0.441969	0.094	0.123
9	N	0.163284	0.442003	0.096	0.126
10	N	0.163291	0.441969	0.118	0.155
Total spin		1.00000	1.00000	0.761	1.000

Qualitatively, the spin density contour obtained with the MP2 method is closer to the picture obtained experimentally using neutron diffraction [21], as it better reveals the presence of a positive spin density in the median space between the central carbons. Quantitatively, however, the DFT method gives values that are closer to the experimental ones, especially if we normalize the total spin contribution to one electron spin.

3.2. Neutral and reduced HCBD

Similar calculations were performed for the HCBD molecule and the $HCBD^{\cdot-}$ anionic radical. After the geometry optimization, it was found that the HCBD molecule is not planar, a twist occurring between the two central double bonds. This result is consistent with experimental data indicating [26] a 140.1^{o} torsion angle about the central C-C bond (about 40^{o} away from the trans morphology). More details regarding the results of the optimization will be presented elsewhere [27]. Here we note that the HOMO of HCBD (Fig. 4a) has π bonds consistent with the structure given in Fig. 1b, while the LUMO (Fig. 4b) has nodal points where the HOMO has bonds and bonds where the HOMO has nodal points. Just like in the case of TCNE, both DFT and MP2 methods give very similar results for the HOMO and the LUMO, but unlike TCNE the results for the next lowest unoccupied MO differ only slightly (Fig. 4c and 4d).

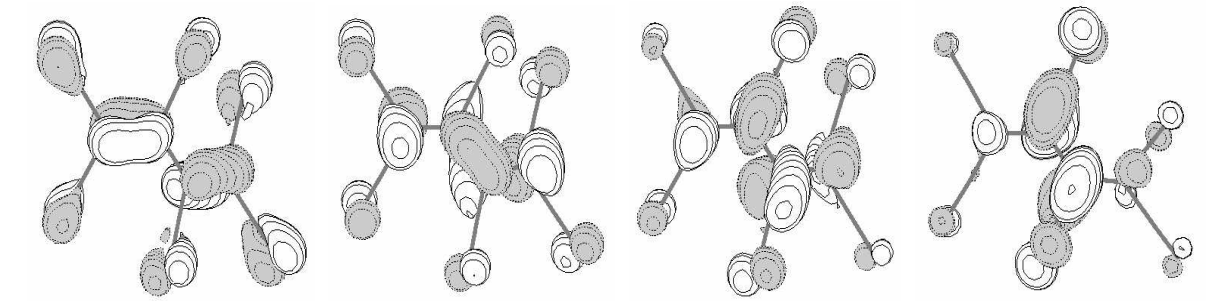

a) b) c) d)

Fig. 4. Electronic density contours (0.002 e/bohr^3) for the highest occupied MO (a), lowest unoccupied MO (b), and next lowest unoccupied MO of HCBD, calculated with DFT (c) and with MP2 (d).

In the case of the anionic radical the SOMO corresponds to the LUMO of the HCBD molecule and the presence of a net spin leads to a difference between the energies for the alpha and beta states. DFT and MP2 give similar results for both the HOMO and the SOMO of $HCBD^{\cdot-}$, results that are very much alike with the HOMO and LUMO of HCBD. Only slight, differences occur when looking further, at the LUMO of the radical.

The adiabatic electron affinity, calculated as the energy difference between the neutral molecule and the anionic radical, is 1.87 eV with MP2/cc-pVDZ and 3.99 eV with DFT/cc-pVDZ. A previous SCF calculation, using a smaller basis set provided a value of 3.21 eV [26]. Just as for $TCNE^{\cdot-}$ MP2 heavily underestimates the affinity. On the other hand, although DFT may tend to overestimate the electron affinity [12,15], it is likely that the true affinity is whithin the estimated error of about 0.3 eV.

The spin distribution of the anionic radical $HCBD^{\cdot-}$ calculated with both DFT and MP2 is shown in Fig. 6. The largest spin density is located on the end carbon atoms of the butadiene backbone and on the nitrogens of the cyano groups. An opposite orientation spin density is located on the carbon atoms that belong to the cyano groups. MP2 calculations give a much smaller density in the middle of the radical, but the topology of the spin density distribution is similar to the one obtained with DFT.

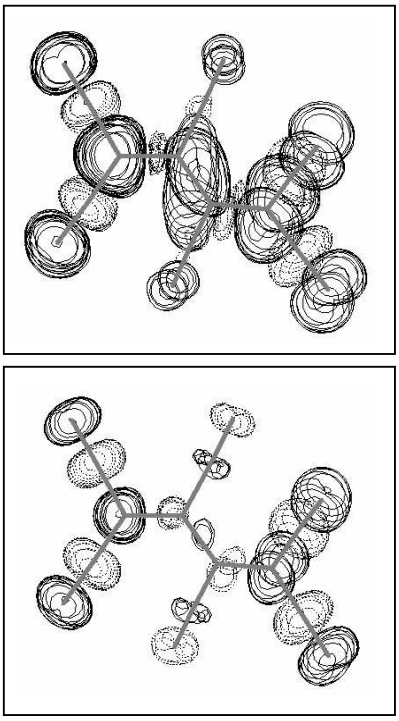

Fig. 6. Spin density contours calculated with DFT (0.002 μ_B/bohr^3) (a) and MP2 (0.01 μ_B/bohr^3) (b).

The spin density distribution of $HCBD^{\cdot-}$ shows interesting similarities with that of $TCNE^{\cdot-}$, exhibiting the same alternation in spin polarization when moving from the nitrogen atoms towards the central part of the radical. Also, the same opposite spin density in the middle of the double bond is observed. The relatively high spin density at the end atoms facilitates the virtual spin transfer in the hybrid organic-inorganic molecular magnets making possible a high kinetic exchange and, therefore, a large superexchange coupling constant.

4. Conclusions

We reported quantum chemical calculations providing the electron affinity and spin density of TCNE, HCBD and their anionic radicals. We used MP2 and DFT calculations to optimize their geometry and determine the electronic structure of the neutral molecules as well as of the anionic radicals. We showed that the TCNE molecule is planar while the HCBD molecule has about 40^o rotation with respect to the trans structure. Also, we found that while the MP2/cc-pVDZ method heavily underestimates the electron affinity (1.70 eV for TCNE and 1.87 eV for HCBD), the DFT/cc-pVDZ technique leads to overestimates (3.10 eV for TCNE and 3.99 eV for HCBD). Although the error is still relatively high (somewhere between 0.2 and 0.5 eV), the DFT method is clearly more precise than MP2 when providing the electron affinity.

The spin density distributions of $TCNE^{\cdot-}$ and $HCBD^{\cdot-}$ show clear similarities, with the same alternation in spin polarization when moving from the nitrogen atoms towards the central part of the radical. For both radicals, the largest spin density is located arround the carbon atoms at the end of the main backbone, while an opposite spin distribution is located in the middle of the double bond.

Discussing our results we speculate that the relatively high spin density at the end atoms facilitates the virtual spin transfer in the hybrid organic-inorganic molecular magnets making possible a high kinetic exchange and, therefore, a large superexchange coupling constant.

Acknowledgements

This work was supported in part by the Romanian Ministry of Education and Research through a PNCDI-INFOSOC research grant 131/20.08.2004. Also, one of the authors, M. A. Gîrţu, gratefully acknowledges the financial support received from Copy**Ro** - The Romanian Society for Reproduction Rights, through the research grant 1636/2004.

References

[1] H. S. Nalwa (Ed.), Handbook of Organic Conductinve molecules and Polymers, vol. **1**, Wiley, Chichester, 1997.
[2] J. S. Miller, A. J. Epstein, Chem. Commun. 1319 (1998).
[3] M. A. Girtu, Hybrid Organic-Inorganic Nanostructured Magnets, in Magnetic Nanostructures, H. S. Nalwa, (Ed.), American Scientific Publishers, Stevenson Ranch, CA, 2001.
[4] C. M. Wynn, M. A. Girtu, W. B. Brinckerhoff, K -I. Sugiura, J. S. Miller, A. J. Epstein, Chem. Mater. **9**, 2156 (1997); C. M. Wynn, M. A. Girtu, K - I. Sugiura, E. J. Brandon, J. L. Manson, J. S. Miller, A .J. Epstein, Synth. Met. **85**, 1695 (1997).
[5] C. M. Wynn, M. A. Girtu, J. S. Miller, A. J. Epstein, Phys. Rev. B. **56**, 14050 (1997).
[6] C. M. Wynn, M. A. Girtu, J. S. Miller, A. J. Epstein, Phys. Rev. B **56**, 315 (1997).
[7] M. A. Girtu, C. M. Wynn, W. Fujita, K. Awaga, A. J. Epstein, J. Appl. Phys. **83**, 7378 (1998); S. J. Etzkorn, W. Hibbs, J. S. Miller, A. J. Epstein, Phys. Rev. Lett. **89**, 207201 (2002).
[8] J. Simons, K. D. Jordan, Chem. Rev. **87**, 535 (1987).
[9] J. C. Rienstra-Kiracofe, G. S. Tschumper, H. F. Schaefer, S. Nandi, G. B. Ellison, Chem. Rev. **102**, 231 (2002).
[10] S. Chowdhury, P. Kebarle J. Am. Chem. Soc. **108**, 5453 (1998).
[11] E. C. Chen, W. E. Wentworth, J. Chem. Phys. **63**, 3183 (1975).
[12] S. T. Brown, J. C. Rienstra-Kiracofe, H. F. Schaefer, J. Phys. Chem. A **103**, 4065 (1999).
[13] N. R. Brinkmann, J. C. Rienstra-Kiracofe, H. F. Schaefer, Mol. Phys. **99**, 663 (2001).

[14] I. Garcia-Cuesta, A. M. J. Sanchez de Meras, H. Koch, J. Chem Phys. **118**, 8216 (2003).
[15] B. Milian, R. Pou-Amerigo, R. Viruela, E. Orti, Chem. Phys. Lett. **375**, 376 (2003).
[16] A. D. Becke, J. Chem. Phys **98**, 5648 (1993).
[17] C. Lee, W. Yang, R. G. Parr, Phys. Rev. B **37**, 785 (1988).
[18] T. H. Dunning Jr., J. Chem. Phys. **90**, 1007 (1989).
[19] GAUSSIAN 03, Revision C.02, M. J. Frisch, et al., Gaussian, Inc., Wallingford CT, 2004.
[20] R. G. Little, D. Pautler, P. Coppens, Acta Cryst. B **27**, 1493 (1973).
[21] A. Zheludev, A. Grand, E. Ressouche, J. Schweizer, B. G. Morin, A. J. Epstein, D. A. Dixon, J. S. Miller, J. Am. Chem. Soc. **116**, 7243 (1994).
[22] MOLDEN 4.4, G. Schaftenaar, CMBI, Nijmegen, The Netherlands, 2005.
[23] P. Becker, P. Coppens, F. K. Ross, J. Am. Chem. Soc. **95**, 7604 (1973).
[24] J. S. Miller, J. C. Calabrese, H. Rommelmann, S. R. Chittipeddi, J. H. Zhang, W. M. Reiff, A. J. Epstein, J. Am. Chem. Soc. **109**, 769 (1987).
[25] D. A. Dixon, J. S. Miller, J. Am. Chem. Soc. **109**, 3656 (1987).
[26] J. S. Miller, J. C. Calabrese, D. A. Dixon, J. Phys. Chem. **95**, 3139 (1991).
[27] C. I. Oprea, A. Damian, M. A. Girtu, to be published.

* Corresponding auhtor: girtu@univ-ovidius.ro